Available online at www.sciencedirect.com
SCIENCE DIRECT®
Carbohydrate Research 338 (2003) 393–398
CARBOHYDRATE RESEARCH
www.elsevier.com/locate/carres

Rapid Communication

Molecular dynamics simulations of an oligosaccharide using a force field modified for carbohydrates☆

Robert Eklund, Göran Widmalm*

Department of Organic Chemistry, Arrhenius Laboratory, Stockholm University, S-106 91 Stockholm, Sweden

Received 4 September 2002; accepted 26 November 2002

Abstract

Parameterization of the ϕ and ω torsion angles in pyranosidic saccharides was performed based on density functional theory calculations. The modified CHARMM force field, which is referred to as PARM22/SU01, was tested on a glucosyl trisaccharide. A molecular dynamics simulation of the oligosaccharide with explicit water as solvent was performed to investigate the conformational flexibility. Proton–proton distances and heteronuclear spin–spin coupling constants were calculated from the trajectories and showed good agreement to those previously determined by NMR spectroscopy. © 2003 Elsevier Science Ltd. All rights reserved.

Keywords: Molecular mechanics; CHARMM; Conformation; Density functional theory; NMR

In biochemical processes carbohydrates are of great importance and form glycoconjugates such as glycoproteins and glycolipids.[1] The understanding of regulation, trafficking and disorders in biological systems relies on knowledge of molecular structure as well as the dynamics. For small to medium-sized systems in solution, NMR spectroscopy is probably the most important technique, whereas for very large systems X-ray crystallography is the method of choice and in the future also solid state NMR spectroscopy. These techniques depend on interpretation of experimental data into a molecular structure. Thus, molecular modeling techniques based on molecular mechanics are usually employed in the structure generation process. To describe the potential energy of the system a force field is used with explicit terms for bonds, angles, torsion angles, etc. Since the original description of the Ramachandran map for peptides,[2] molecular mechanics approaches in the field of carbohydrates have been developed continuously.[3–6] However, the detailed description of the conformation and dynamics at the glycosidic linkage is still a problem of considerable difficulty. In the present communication we describe modifications to a CHARMM-based force field for the improvement of parameters to be used in the modeling of carbohydrate structures.

In our analysis of oligosaccharide conformation we have employed Monte Carlo, Langevin dynamics and Molecular dynamics (MD) simulation techniques in conjunction with several different force fields.[7] In one of our recent studies of a trisaccharide it was evident from experimental NMR data that the PARM22 force field,[8] which is a CHARMM22 type of force field,[9] overestimated the population of an *anti*-ϕ torsion angle.[10] Furthermore, from a comparison of the ab initio calculated potential energy difference for the equatorial con-

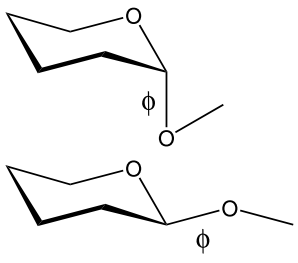

Fig. 1. Schematic of the axial 2MTHP (top) and the equatorial 2MTHP (bottom).

☆ Presented at the 223rd American Chemical Society National Meeting, Orlando, FL, USA, April 7–11, 2002.

* Corresponding author. Tel.: +46-81-63742; fax: +46-81-54908

E-mail address: gw@organ.su.se (G. Widmalm).

PII: S0008-6215(02)00503-7

Table 1
Torsional angles of ϕ (°) in 2MTHP and the relative energies (kcal mol^{-1}) calculated by DFT

ϕ_{axial}	Relative energy	$\phi_{equatorial}$	Relative energy
9.30	3.56	6.21	3.10
19.30	3.67	16.21	2.29
29.30	3.67	26.21	1.38
39.30	3.67	36.21	0.57
49.30	3.79	46.21	0.06
59.30	4.08	56.21	0.00 [b]
69.30	4.59	66.21	0.44
79.30	5.31	76.21	1.31
89.30	6.21	86.21	2.44
99.30	7.22	96.21	3.61
109.30	8.20	106.21	4.58
119.30	8.90	116.21	5.14
129.30	9.08	126.21	5.18
139.30	8.89	136.21	4.75
149.30	8.67	146.21	4.05
159.30	8.50	156.21	3.35
169.30	8.49	166.21	2.93
179.30	8.57	176.21	2.80
189.30	8.65	186.21	2.97
199.30	8.78	196.21	3.50
209.30	8.91	206.21	4.34
219.30	8.97	216.21	5.34
229.30	8.86	226.21	6.34
239.30	8.40	236.21	7.09
249.30	7.54	246.21	7.39
259.30	6.12	256.21	7.23
269.30	4.27	266.21	6.76
279.30	2.48	276.21	6.13
289.30	1.09	286.21	5.49
299.30	0.26	296.21	4.94
309.30	0.00 [a]	306.21	4.56
319.30	0.24	316.21	4.35
329.30	0.83	326.21	4.26
339.30	1.65	336.21	4.21
349.30	2.50	346.21	4.06
359.30	3.18	356.21	3.70

[a] Absolute energy = −386.3139757 Hartree.
[b] Absolute energy = −386.3126641 Hartree.

formation of 2-methoxytetrahydropyran (2MTHP) it was noted that for a CHARMM-based force field the relative energy difference at the ϕ torsion angle between the *syn* and the *anti* conformations was too low.[11] We therefore set out to reparameterize the PARM22 force field.

As a model we, like others,[12] chose the axial and equatorial conformations of 2MTHP shown in Fig. 1. Structures were geometry optimized using density functional theory (DFT) calculations[13] at the B3LYP/6-31 + G(d) level of theory[14,15] (Table 1). It should be noted that for complex molecules it is difficult to predict relative energy differences between different basis sets[12] and that for studying intramolecular hydrogen bonding a high level calculation is a prerequisite for reliable results.[16] In the present study the above described level of theory should suffice as applied to 2MTHP. The potential energy curves for rotation of the ϕ torsion angle are shown in Fig. 2. The energy minima for the axial and equatorial conformations of 2MTHP are present in staggered forms known as the *exo*-anomeric conformation.[17] The force constants were optimized using three different terms, applicable to both the axial and equatorial forms of 2MTHP (Table 2). The molecular mechanics derived torsions agree well with those from DFT (Fig. 2).

The conformational preference of the exocyclic hydroxymethyl group in hexopyranosides is an important and intricate problem in carbohydrate chemistry.[18–20] During the development of the ϕ torsional parameters, a study on various aspects of the ω torsion angle in hexopyranosides was published[21] and since we had observed that the *gt* conformation in glucosyl residues was over represented in the PARM22 force field,[22] we decided to modify the torsional terms also for this angle. The repulsive quantum mechanical potential energy data for rotation of the ω torsion angle are shown for α-D-Glc*p*-OMe (Fig. 2c) and α-D-Gal*p*-OMe (Fig. 2d).

Herein, the force constants for the O-5–C-5–C-6–O-6 torsion were parameterized using the repulsive part of the ω torsion, that is, with the C-5–C-6–O-6–HO-6 torsion restrained in a *trans* conformation, so that internal hydrogen bonding, between HO-6 and O-5, was not possible. Kirschner and Woods showed that the repulsive part of the potential energy curves differed significantly, whereas the attractive part with internal hydrogen bonding was similar for the two sugars and that for the attractive part the populations of the ω torsions were not in agreement with experimental data.[21]

The results for the parameterization of the force field in CHARMM, using the same torsional description for both α-D-Glc*p*-OMe and α-D-Gal*p*-OMe, are shown in Fig. 2 and the force constants for the three torsional terms are given in Table 2. Thus, we have parameterized three key torsion angles in pyranosidic hexoses to be used for oligo- and polysaccharides. We now test this modification of the CHARMM force field referred to as PARM22/SU01 (the latter denotes Stockholm University, year 01).

For the trisaccharide β-D-Glc*p*-(1→2)[β-D-Glc*p*-(1→3)]-α-D-Glc*p*-OMe (**1**) (Fig. 3) we have previously obtained a good deal of data from solution state NMR spectroscopy, including ^{13}C relaxation parameters, ^{1}H,^{1}H cross-relaxation rates which give internuclear distances[23] and *trans*-glycosidic $^{3}J_{C,H}$ values which can be interpreted via a Karplus-type relationship.[24]

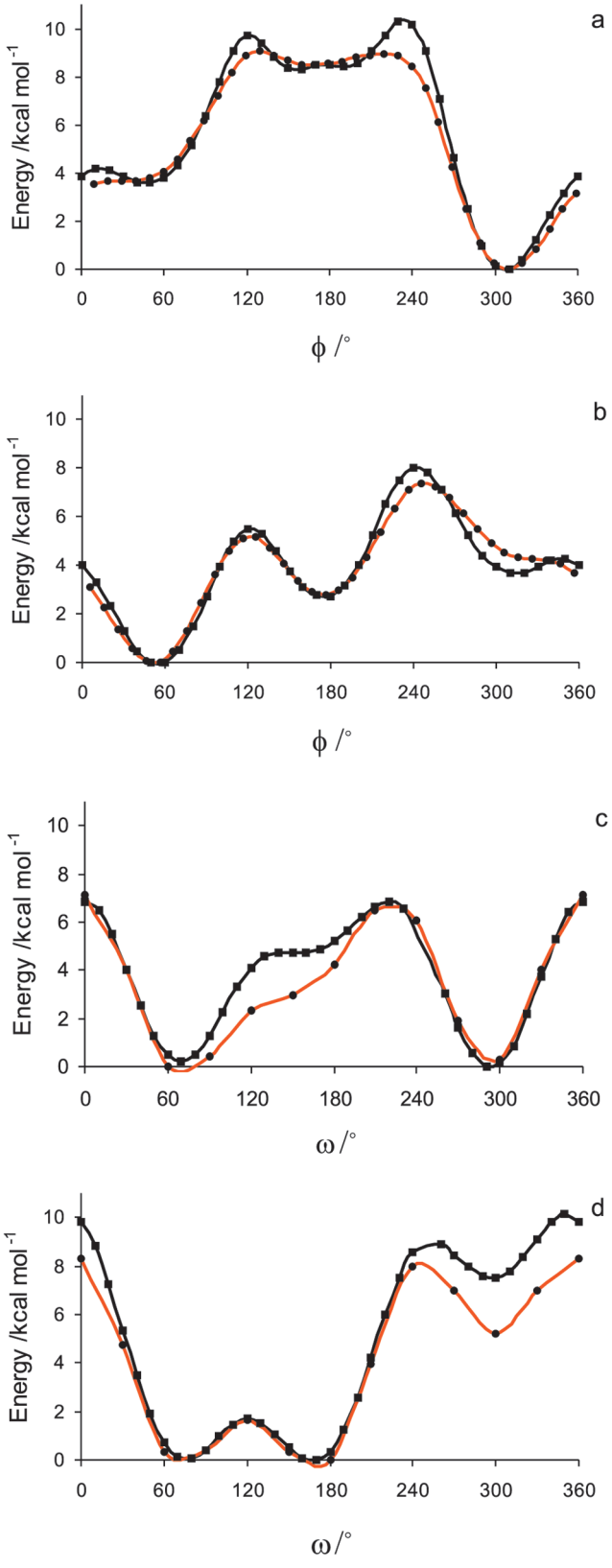

Fig. 2. Potential energy curves of ϕ in: (a) axial 2MTHP; (b) equatorial 2MTHP; and ω in (c) α-D-Glc*p*-Ome; and (d) α-D-Gal*p*-OMe calculated by DFT (●) or the derived PARM22/SU01 molecular mechanics (■) methods.

A molecular dynamics simulation of **1** employing PARM22/SU01 with explicit TIP3P water molecules was performed for 5 ns. Torsion angle averages were calculated ($\langle\phi_2\rangle = 39$, $\langle\psi_2\rangle = -37$, $\langle\phi_3\rangle = 42$, $\langle\psi_3\rangle = 4°$) as well as interproton distances and $^3J_{C,H}$ values (Table 3 and Table 4). The scatter plots of the MD simulation for the (1→2)- and (1→3)-linked glucosyl groups of the trisaccharide are shown in Fig. 4. It should be noted that the ψ torsion angles differ by $\sim 40°$, whereas the ϕ torsion angles are very similar. Thus, the conformational preference at the two glycosidic linkages differ. Still, the agreement with experimental *trans*-glycosidic proton distances is very good (Fig. 5 and Table 3). In our previous study we utilized, inter alia, the PARM22 force field for **1** but the proton distances calculated from simulation were significantly longer than in the present simulation with the PARM22/SU01 force field thereby lending credence to the modifications performed herein. In addition, the $^3J_{C,H}$ values related to the ϕ torsions are well reproduced in the simulation and the trends for the $^3J_{C,H}$ values of ψ are correct, i.e., larger at the β-(1→3)-linkage than at the β-(1→2)-linkage. Moreover, a comparison to the *trans*-glycosidic proton distances in the crystal structure, reveals that the conformational preference in solution is similar to that in the crystal.

Transitions between different rotamers of the hydroxymethyl group in hexopyranosides have recently been shown to occur on the short nanosecond time scale.[25] Although the present simulation is far too short to obtain well converged results on the population distribution and transition rates for ω the torsion angle we note that transitions occur on the appropriate time scale (Fig. 6).

In conclusion, the parameterization of the ϕ and ω torsion angles for a CHARMM force field showed good agreement to experimental NMR data. Thus, the description of saccharide flexibility and dynamics is improved and facilitates future studies in conjunction with carbohydrate binding proteins or glycoproteins per se. It is anticipated that a similar protocol can be performed for other CHARMM-based force fields[9] and that a comparison to recent force field developments[26–28] will lead to an understanding of and a consensus on oligosaccharide flexibility and dynamics.

1. Methods

Molecular mechanics and molecular dynamics simulations were performed with the CHARMM program[8,29] running on an SGI O_2 workstation or an IBM SP2 computer (parallel version 27b4). DFT calculations were carried out with the GAUSSIAN-98 program[30] (Revision A.7) on the same IBM SP2 computer. 2MTHP molecules were built with the MOLDEN program[31] and

Table 2
Torsional force constants (kcal mol^{-1})

Type	V_1	V_2	V_3
CT-CT-OE-CT	1.2	0.0	0.25 [a]
OE-CT-OE-CT	1.2	1.0	0.9
OT-CT-CT-OE	−3.4 (δ 200) [b]	1.3	0.5

[a] As in PARM22.
[b] δ = phase factor in degrees.

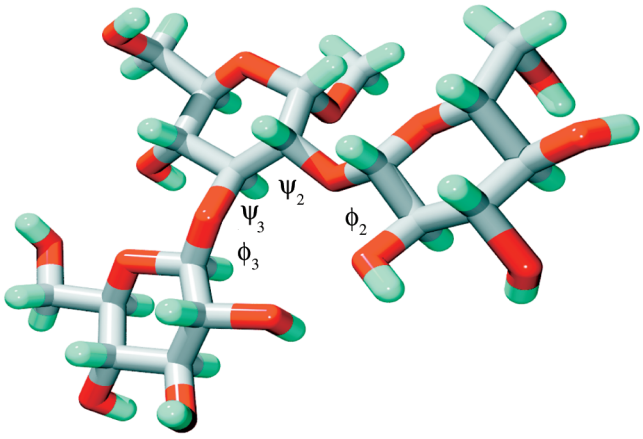

Fig. 3. Crystal structure of β-D-Glc*p*-(1→2)[β-D-Glc*p*-(1→3)]-α-D-Glc*p*-OMe (**1**) showing the glycosidic torsion angles, where the linkage positions are identified by subscripts.

Table 3
Comparison of proton distances (Å) from simulation and experiment for trisaccharide **1**

Protons	MD [a]	NMR [b]	Crystal
1g–2g	2.42	2.42 [c]	2.27
2g–1g^2	2.28	2.25	2.11
3g–1g^3	2.29	2.26	2.26
1g–1g^2	3.01	3.16	3.03

[a] Averaged according to $r = \langle r^{-3} \rangle^{-1/3}$.
[b] Calculated using the Isolated Spin Pair Approximation and ^{1}H,^{1}H NOE and T-ROE data obtained in D_2O.[23]
[c] Reference distance from MD simulation.

exported to GAUSSIAN-98 where the structures were geometry optimized to find the global energy minimum. The DFT calculations were performed at the B3LYP/6-31 + G(d) level of theory using standard convergence criteria in GAUSSIAN-98. Subsequent torsional rotations were carried out in 10° increments with the command *frozen* to obtain geometry optimized structures. Rotations in CHARMM were performed by restraining the H1–C1–O1–CM torsion by a force constant of 1000 kcal mol^{-1} followed by 10 steps of steepest descent energy minimization and an adopted basis Newton–Raphson minimization for 1000 steps or until the rms gradient was less than 10^{-4} kcal mol^{-1} Å^{-1}. Discrepancies between the PARM22 results and the DFT data were readily identified by inspection. Subsequently, the force constants for the torsional terms in 2MTHP and the methyl hexopyranosides were optimized in a heuristic manner until the fit of the molecular mechanics potential energy curves was in good agreement with the DFT data (cf. Fig. 2). The torsional curves were visualized with the MATLAB program[32] (version 5.3).

The MD simulation of **1** was performed with a dielectric constant of unity and a time step of 1 fs in a cubic box of water 29.97 Å to the side containing 855 TIP3P water molecules. After heating and equilibration (~200 ps) a production run was performed for 5 ns at

Table 4
Comparison of heteronuclear *trans*-glycosidic spin–spin coupling constants (Hz) from simulation and NMR experiment of trisaccharide **1**

Atoms	MD [a]	NMR [b]
H1g^2–C2g	3.9	3.8
C1g^2–H2g	3.7	4.5
H1g^3–C3g	3.6	3.9
C1g^3–H3g	6.0	4.9

[a] Calculated using $^3J_{C,H} = 7.49 \cos^2\theta - 0.96 \cos\theta + 0.15$.[35]
[b] $^3J_{C,H}$ data obtained in D_2O.[24]

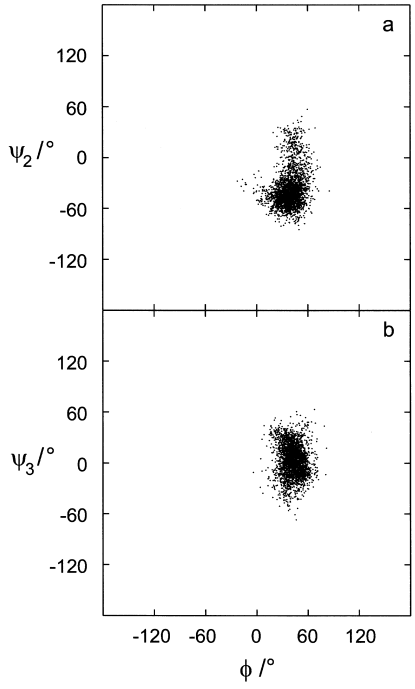

Fig. 4. Scatter plots from the MD simulation of **1** showing the ϕ/ψ distributions of: (a) the β-(1→2)-linkage; and (b) the β-(1→3)-linkage.

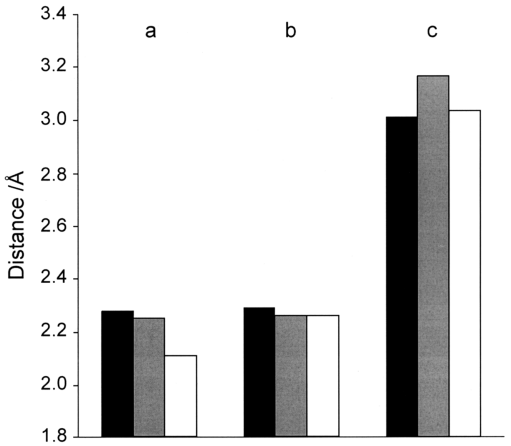

Fig. 5. Comparison of proton–proton distances (Å) in **1** showing: (a) $H1g^2$–H2g; (b) $H1g^3$–H3g; and (c) $H1g^2$–H1g. Data from MD simulation (black), NMR experiment (gray) and the crystal structure (white). The superscripts of the terminal glucosyl residues refer to the substitution position at the α-D-Glc*p* residue.

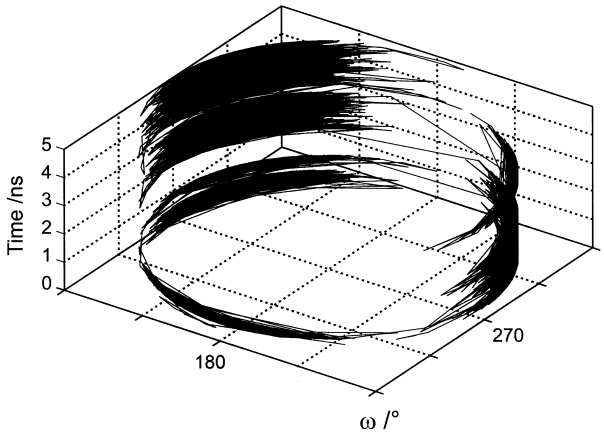

Fig. 6. MD trajectory of the ω torsion angle of the α-D-Glc*p* residue in **1**.

300 K, in which the temperature was scaled by Berendsen's weak coupling algorithm.[33] Minimum image boundary conditions were used with a heuristic nonbond frequency update and a force shift cutoff acting to 12 Å.[34]

Acknowledgements

This work was supported by a grant from the Swedish Research Council. We thank the Center for Parallel Computers, KTH, Stockholm, for putting computer facilities at our disposal.

References

1. Varki, A.; Cummings, R.; Esko, J.; Freeze, H.; Hart, G.; Marth, J., Eds. *Essential of Glycobiology*; Cold Spring Harbor Laboratory Press: Cold Spring Harbor, NY, 1999.
2. Ramachandran, G. N.; Sasisekharan, V.; Ramakrishnan, C. *J. Mol. Biol.* **1963**, *7*, 95–99.
3. Brant, D. A. *Annu. Rev. Biophys. Bioeng.* **1972**, *1*, 369–408.
4. Ha, S. N.; Giammona, A.; Field, M.; Brady, J. W. *Carbohydr. Res.* **1988**, *180*, 207–221.
5. Woods, R. J. In *Encyclopedia of Computational Chemistry*; von Ragué Schleyer, P., Ed.; John Wiley & Sons: Chichester, 1998; pp 220–233.
6. Peréz, S.; Imberty, A.; Engelsen, S. B.; Gruza, J.; Mazeau, K.; Jiménez-Barbero, J.; Poveda, A.; Espinosa, J. F.; van Eyck, B. P.; Johnson, G.; French, A. D.; Kouwijzer, M. L. C. E.; Grootenuis, P. D. J.; Bernardi, A.; Raimondi, L.; Senderowitz, H.; Durier, V.; Vergoten, G.; Rasmussen, K. *Carbohydr. Res.* **1998**, *314*, 141–155.
7. Lycknert, K.; Höög, C.; Widmalm, G. *J. Chem. Soc., Perkin Trans. 2* **2002**, 416–421.
8. Accelrys Inc. http://www.accelrys.com/ (accessed June 2002).
9. MacKerell, A. D., Jr.; Bashford, D.; Bellott, M.; Dunbrack, R. L., Jr.; Evanseck, J. D.; Field, M. J.; Fischer, S.; Gao, J.; Guo, H.; Ha, S.; Joseph-McCarthy, D.; Kushnir, L.; Kuczera, K.; Lau, F. T. K.; Mattos, C.; Michnick, S.; Ngo, T.; Nguyen, T. D.; Prodhom, B.; Reiher, W. E., III; Roux, B.; Schlenkrich, M.; Smith, J. C.; Stote, R.; Straub, J.; Watanabe, M.; Wiórkiewicz-Kuczera, J.; Yin, D.; Karplus, M. *J. Phys. Chem., B* **1998**, *102*, 3586–3616.
10. Höög, C.; Landersjö, C.; Widmalm, G. *Chem. Eur. J.* **2001**, *7*, 3069–3077.
11. Tvaroska, I.; Carver, J. P. *J. Phys. Chem.* **1994**, *98*, 9477–9485.
12. Momany, F. A.; Willett, J. L. *J. Comput. Chem.* **2000**, *21*, 1204–1219.
13. Koch, W.; Holthausen, M. C. *A Chemist's Guide to Density Functional Theory*; Wiley-VCH: Weinheim, 2000.
14. Becke, A. D. *J. Chem. Phys.* **1993**, *98*, 5648–5652.
15. Lee, C.; Yang, W.; Parr, R. G. *Phys. Rev. B* **1988**, *37*, 785–789.
16. Lii, J.-H.; Ma, B.; Allinger, N. L. *J. Comput. Chem.* **1999**, *20*, 1593–1603.
17. *The Anomeric Effect and Associated Stereoelectronic Effects*; Thatcher, G. R. J., Ed.; American Chemical Society: Washington DC, 1993.
18. Rockwell, G. D.; Gindley, T. B. *J. Am. Chem. Soc.* **1998**, *120*, 10953–10963.
19. Stenutz, R.; Carmichael, I.; Widmalm, G.; Serianni, A. S. *J. Org. Chem.* **2002**, *67*, 949–958.
20. Tvaroska, I.; Taravel, F. R.; Utille, J. P.; Carver, J. P. *Carbohydr. Res.* **2002**, *337*, 353–367.
21. Kirschner, K. N.; Woods, R. J. *Proc. Nat. Acad. Sci. USA* **2001**, *98*, 10541–10545.
22. Höög, C.; Widmalm, G. *Arch. Biochem. Biophys.* **2000**, *377*, 163–170.
23. Rundlöf, T.; Eriksson, L.; Widmalm, G. *Chem. Eur. J.* **2001**, *7*, 1750–1758.
24. Rundlöf, T.; Kjellberg, A.; Damberg, C.; Nishida, T.; Widmalm, G. *Magn. Reson. Chem.* **1998**, *36*, 839–847.
25. Stenger, J.; Cowman, M.; Eggers, F.; Eyring, E. M.; Kaatze, U.; Petrucci, S. *J. Phys. Chem., B* **2000**, *104*, 4782–4790.
26. Palma, R.; Zuccato, P.; Himmel, M. E.; Liang, G.; Brady, J. W. In *Glycoyl Hydrolases for Biomass Conversion*; Himmel, M. E.; Baker, J. O.; Saddler, J. N., Eds.; ACS Symp. Ser., Vol. 769; ACS: Washington, DC, 2001; pp 112–130.

27. Kuttel, M.; Brady, J. W.; Naidoo, K. N. *J. Comput. Chem.* **2002**, *23*, 1236–1243.
28. Kony, D.; Damm, W.; Stoll, S.; van Gunsteren, W. F. *J. Comput. Chem.* **2002**, *23*, 1416–1429.
29. Brooks, B. R.; Bruccoleri, R. E.; Olafson, B. D.; States, D. J.; Swaminathan, S.; Karplus, M. *J. Comput. Chem.* **1983**, *4*, 187–217.
30. Frisch, M. J.; Trucks, G. W.; Schlegel, H. B.; Scuseria, G. E.; Robb, M. A.; Cheeseman, J. R.; Zakrzewski, V. G.; Montgomery, J. A., Jr.; Stratmann, R. E.; Burant, J. C.; Dapprich, S.; Millam, J. M.; Daniels, A. D.; Kudin, K. N.; Strain, M. C.; Farkas, O.; Tomasi, J.; Barone, V.; Cossi, M.; Cammi, R.; Mennucci, B.; Pomelli, C.; Adamo, C.; Clifford, S.; Ochterski, J.; Petersson, G. A.; Ayala, P. Y.; Cui, Q.; Morokuma, K.; Malick, D. K.; Rabuck, A. D.; Raghavachari, K.; Foresman, J. B.; Cioslowski, J.; Ortiz, J. V.; Baboul, A. G.; Stefanov, B. B.; Liu, G.; Liashenko, A.; Piskorz, P.; Komaromi, I.; Gomperts, R.; Martin, R. L.; Fox, D. J.; Keith, T.; Al-Laham, M. A.; Peng, C. Y.; Nanayakkara, A.; Gonzalez, C.; Challacombe, M.; Gill, P. M. W.; Johnson, B. G.; Chen, W.; Wong, M. W.; Andres, J. L.; Gonzalez, C.; Head-Gordon, M.; Replogle, E. S.; Pople, J. A. GAUSSIAN-98, revision A.7; GAUSSIAN, Inc.: Pittsburgh, PA, 1998.
31. Schaftenaar, G. MOLDEN, CMBI, The Netherlands. http://www.cmbi.kun.nl/~schaft/molden/molden.html (accessed June 2002).
32. The Mathworks, Inc. http://www.mathworks.com/ (accessed June 2002).
33. Berendsen, H. J. C.; Postma, J. P. M.; van Gunsteren, W. F.; DiNola, A.; Haak, J. R. *J. Chem. Phys.* **1984**, *81*, 3684–3690.
34. Steinbach, P. J.; Brooks, B. R. *J. Comput. Chem.* **1994**, *15*, 667–683.
35. Cloran, F.; Carmichael, I.; Serianni, A. S. *J. Am. Chem. Soc.* **1999**, *121*, 9843–9851.